Received: 18 March 2024 | Revised: 13 May 2024 | Accepted: 17 June 2024

DOI: 10.1002/alz.14125

Alzheimer's & Dementia®
THE JOURNAL OF THE ALZHEIMER'S ASSOCIATION

RESEARCH ARTICLE

Synaptic and extrasynaptic distribution of NMDA receptors in the cortex of Alzheimer's disease patients

Sergio Escamilla[1,2,3] | **Raquel Badillos**[2,4,5] | **Joan X. Comella**[2,4,5,6] | **Montse Solé**[2,4,5] | **Isabel Pérez-Otaño**[1] | **Jose V. Sánchez Mut**[1] | **Javier Sáez-Valero**[1,2,3] | **Inmaculada Cuchillo-Ibáñez**[1,2,3]

[1]Instituto de Neurociencias, Universidad Miguel Hernández-Consejo Superior de Investigaciones Científicas (UMH-CSIC), Sant Joan d'Alacant, Spain

[2]Centro de Investigación Biomédica en Red sobre Enfermedades Neurodegenerativas (Ciberned), Madrid, Spain

[3]Instituto de Investigación Sanitaria y Biomédica de Alicante (Isabial), Alicante, Spain

[4]Departament de Bioquímica i Biologia Molecular, School of Medicine, Universitat Autònoma de Barcelona (UAB), Bellaterra (Barcelona), Spain

[5]Institut de Neurociències, Universitat Autònoma de Barcelona (UAB), Bellaterra (Barcelona), Spain

[6]Institut de Recerca Sant Joan de Déu, Hospital Sant Joan de Déu, Esplugues de Llobregat, Spain

Correspondence
Inmaculada Cuchillo-Ibáñez and Javier Sáez-Valero, Instituto de Neurociencias, Universidad Miguel Hernández-Consejo Superior de Investigaciones Científicas (UMH-CSIC), 03550 Sant Joan d'Alacant, Spain.
Email: icuchillo@umh.es and j.saez@umh.es

Funding information
Fondo de Investigaciones Sanitarias, co-funded by the Fondo Europeo de Desarrollo Regional, FEDER "Investing in your future, Grant/Award Number: PI22/01329; Direcció General de Ciència i Investigació, Generalitat Valenciana, Grant/Award Number: AICO/2021/308; Centro de Excelencia Severo Ochoa, Agencia Estatal de Investigación, Grant/Award Number: CEX2021-001165-S; Instituto de Investigación Sanitaria y Biomédica de Alicante (Isabial); Programa Investigo, Conselleria de Innovación, Universidades, Investigación y Sociedad Digital, , Generalitat Valenciana, Grant/Award Number: INVEST-2023-157; CIBERNED (Instituto de Salud Carlos III)

Abstract

BACKGROUND: Synaptic and extrasynaptic distribution of N-methyl-D-aspartate receptors (NMDARs) has not been addressed in the brain from Alzheimer´s disease (AD) subjects, despite their contribution to neurodegeneration.

METHODS: We have developed a protocol to isolate synaptic and extrasynaptic membranes from controls and AD frontal cortex. We characterized the distribution of the NMDAR subunits GluN2B, GluN2A, GluN1, and GluN3A, as well as post-translational modifications, such as phosphorylation and glycosylation.

RESULTS: Lower levels of synaptic GluN2B and GluN2A were found in AD fractions, while extrasynaptic GluN2B and GluN1 levels were significantly higher; GluN3A distribution remained unaffected in AD. We also identified different glycoforms of GluN2B and GluN2A in extrasynaptic membranes. Synaptic Tyr1472 GluN2B phosphorylation was significantly lower in AD fractions.

DISCUSSION: Reduction of synaptic NMDAR subunits, particularly for GluN2B, is likely to contribute to synaptic transmission failure in AD. Additionally, the increment of extrasynaptic NMDAR subunits could favor the activation of excitotoxicity in AD.

KEYWORDS
Alzheimer´s disease, extrasynaptic, GluN1, GluN2A, GluN2B, GluN3A, human, NMDA, Tyr1336, Tyr1472

Highlights

- New protocol to isolate synaptic and extrasynaptic membranes from the human cortex.
- Low GluN2B and GluN2A levels in Alzheimer´s disease (AD) synaptic membranes.
- High GluN2B and GluN1 levels in AD extrasynaptic membranes.
- Specific glycoforms of extrasynaptic GluN2B and GluN2A.
- Low phosphorylation at Tyr1472 in synaptic GluN2B in AD.

1 | BACKGROUND

N-Methyl-D-aspartate receptors (NMDARs), cation channels gated by the neurotransmitter glutamate, are essential mediators of synaptic transmission and many forms of synaptic plasticity.[1] NMDARs displays unique properties that depend on their subunit composition, but few studies have employed human brain tissues to examine their distribution.[1] Furthermore, the characterization of NMDAR diversity under neuropathological conditions such as Alzheimer´s disease (AD) has not been fully addressed in human tissue, despite the fact that memantine, a drug that binds weakly to the ion channel, is used in AD therapy.[2]

Functional NMDARs are tetramers composed of different subunits, GluN1, GluN2(A-D), and GluN3(A-B). Endogenous NMDARs are diheteromers composed of two obligatory GluN1 subunits and two GluN2 or GluN3 subunits, which finally assemble as a dimer of dimers[3] although NMDARs are also able to assemble as tri-heteromers.[4] In the brains of adult mice and adult human together with GluN1, the main subunits are GluN2A and GluN2B,[1,5] which have a large N-terminal extracellular domain that contains the binding sites for glutamate and co-agonists D-serine or glycine, necessary for the effective activation of NMDARs.[6] The NMDAR intracellular domains interact with the intracellular post-synaptic density protein-95 (PSD-95) adaptor protein,[7] and the C-terminal of ApoER2, a receptor that binds apolipoprotein E (apoE) and reelin.[8,9] Additionally, NMDAR subunit ectodomains are robustly glycosylated, as N-glycosylation is required for the efficient surface expression of NMDAR in neurons (reviewed in Ref.[10]).

The trafficking and synaptic expression of NMDARs are also tightly regulated by Src a family of protein tyrosine kinases, including Fyn, via direct phosphorylation in tyrosines located within the long intracellular C-terminal domains of GluN2 subunits.[11] Three major tyrosines in the GluN2B C-terminal tail have been identified by site-directed mutagenesis as Fyn phosphorylation sites: Tyr1472, Tyr1336, and Tyr1252. Phosphorylation of GluN2B at Tyr1472[12] strengthens the interaction between NMDARs and PSD-95 and prevents their binding to the endocytic adaptor AP2, enhancing the synaptic clustering and activity of GluN2B-containing NMDARs.[13] Tyr1472 phosphorylation and GluN2B interaction with PSD-95 stabilize NMDAR in the synaptic plasma membrane and prevent it from being endocytosed or translocated to extrasynaptic membranes. GluN2B is also phosphorylated at Tyr1336 by Fyn, an event that has been associated with enrichment of GluN2B-containing receptors in extrasynaptic membranes[14,15] and low colocalization with PSD-95.[16] The role of Tyr1252 phosphorylation is yet unknown.

Synaptic NMDARs are directly involved in excitatory neurotransmission, plasticity, and pro-survival activity, whereas stimulation of extrasynaptic NMDARs causes a loss of mitochondrial membrane potential, an early marker for glutamate-induced neuronal damage, and cell death.[14] Chronic activation of extrasynaptic GluN2B and GluN2A-containing NMDARs leads to excitotoxicity, while the GluN3A subunit is considered preventive against excitotoxicity.[17,18]

Sustained NMDAR hyperactivity and Ca^{2+} dysregulation lasting from months to years is likely related to AD development.[19] In this context, two key proteins for the pathophysiology of the disease, tau, a microtubule-associated protein, and amyloid-β, Aβ, the principal component of senile plaques, have been associated with NMDAR impairment. Dysregulated tau phosphorylation negatively affects synaptic NMDAR-glutamatergic signaling (reviewed in Ref.[20]). Aβ causes NMDAR dysregulation by loss of Ca^{2+} homeostasis, which is related to early cognitive deficits, and both Aβ oligomers and NMDAR impairment contribute to synaptic dysfunction in AD.[21–23]

This study is the first to characterize the levels of GluN2B, GluN2A, GluN1, and GluN3A subunits in the brain of AD subjects, discriminating between synaptic and extrasynaptic membranes and addressing post-translational modifications, specifically phosphorylation, and glycosylation. Analyzing frontal cortices from AD patients and brain cortices from two mice models of AD, Tau301S, and APP/PS1, we now report changes in the distribution of NMDAR subunits between synaptic and extrasynaptic fractions.

2 | METHODS

2.1 | Human brain simples

This study was approved by the ethics committee of both, the Universidad Miguel Hernández de Elche and the Departamento de Salud de Alicante – Hospital General (Spain), and it was carried out in accordance with the WMA Declaration of Helsinki. Brain samples (frontal cortex, Brodmann area 8) and data from patients included in this study were provided by the Biobank HUB-ICO-IDIBELL (PT20/00171),

integrated into the ISC-III Biobanks and Biomodels Platform and they were processed following standard operating procedures with the appropriate approval of the Ethics and Scientific Committees. Cases with AD-related pathology were considered those showing neurofibrillary tangles (NFT) and/or senile plaques with the distribution established by Braak and Braak at the *post mortem* neuropathological examination.[24] These were categorized as Braak stages I–II, $n = 8$, 1 female/7 males, 63 ± 5 years; Braak stages III–IV, $n = 9$, 4 females/5 males, 78 ± 7 years; and Braak stages V–VI, $n = 8$, 3 females/5 males, 76 ± 6 years. Taking together from Braak I–VI $n = 25$, 8 females/17 males, 72 ± 9 years. Cases at stages I, II, and III did not have cognitive impairment; three cases at stage IV had moderate cognitive impairment, and cases at stages V and VI all suffered dementia. Special care was taken not to include cases with combined pathologies to avoid bias in the pathological series. Non-demented subjects, $n = 14$, 4 females/10 males, 56 ± 10 years. The mean *post mortem* interval of the tissue was 7.1 h in all cases, with no significant difference between the subgroups. See Table S1 for summarized details.

2.2 | Mice

The APP/PS1 mouse model of AD initiates Aβ deposits, astrogliosis and learning deficits at 6 months of age, all of which increase with age. In this study APP/PS1 mice of 12 months of age were used ($n = 22$, all males). The TauP301S mouse model of tauopathy accumulate pTau/Tau at 6 months of age in the hippocampus, but until 9 months, when these mice were used, they do not show a decrease in PSD95 and GluR2, and an increase in GFAP, that indicates hippocampal pathology (n male = 13, n female = 17).

2.3 | Subcellular fractionation protocol

Human frozen frontal cortices were cut into pieces (100 mg) trying to avoid white matter and excess of vascular tissue. When the protocol was performed in mouse brain tissue, whole frontal cortices were used (~20 mg). Each piece was homogenized in 100 μL for human samples or 200 μL for mouse samples of homogenization buffer (ice-cold sucrose buffer containing 0.32 M sucrose, 10 mM Tris–HCl (pH 7.4), 1 mM Na_3VO_4, 1 mM NaF, 1 mM HEPES, 1 mM ethylenediaminetetraacetic acid (EDTA), 1 mM EGTA, protease, and phosphatase inhibitors) in a 1.5 mL eppendorf using a Heidolf homogenizer (10 strokes). The subsequent centrifugations were all performed at 4°C. Cortical homogenates (Ho) were centrifuged at 1000×*g* for 10 min to obtain a nuclear-free supernatant (S1) and a pellet (P1) containing the nucleus. Further centrifugation of S1 at 10,000×*g* for 15 min resulted in a supernatant that contained cell cytosol and microsomes (S2) and a pellet (P2) of plasma membranes. P2 was incubated with homogenization buffer containing 1% TX-100 (w/v) for 20 min in rotation at 4°C and then centrifuged at 32,000×*g* for 20 min. The supernatant fraction collected contained extrasynaptic membranes, which include non-synaptic membranes and presynaptic membranes (extrasynaptic fraction, ExsynF); the pellet fraction, containing the insoluble fraction, was solubilized in RIPA buffer. This pellet was mainly composed of post-synaptic densities and therefore, post-synaptic membranes (synaptic fraction, SynF). Finally, ultracentrifugation at 100,000×*g* for 1 h of S2 fraction made it possible to discriminate microsomal (solubilized in RIPA buffer, P3) and cytosolic fractions (S3).

RESEARCH IN CONTEXT

1. **Systematic review**: Unbalanced N-methyl-D-aspartate receptor (NMDAR) distribution in synaptic and extrasynaptic membranes is crucial for Alzheimer's disease (AD). Most evidence accumulated on this topic is based on transgenic models and does not discriminate between synaptic and extrasynaptic membranes. We include these publications and those performed in synaptosomes from the human brain.
2. **Interpretation**: The value of our study lies in the first characterization of NMDAR subunit distribution in the human cortex from controls and AD subjects, with special emphasis on the description of extrasynaptic NMDAR subunits.
3. **Future directions**: Additional studies could address the following questions: (A) We have identified specific glycoforms of GluN2B and GluN2A in extrasynaptic membranes. Further investigation is needed to know whether these subunits are functional and contribute to excitotoxic mechanisms. (B) Some authors point to a decrease of GluN3A subunit in AD, but we observed no changes in its distribution. More studies are needed to clarify its role in AD.

2.4 | Western blotting

Brain fractions were run on sodium dodecyl sulfate-polyacrylamide gel electrophoresis (SDS-PAGE) (7.5% Tris-glycine) after boiling at 98°C for 5 min in 6× Laemmli sample buffer. Proteins were transferred by electrophoresis to nitrocellulose membranes for 1 h at 100 V. Primary antibodies were used against GluN2B C-terminal (mouse, 1:800, Invitrogen MA1-2014), GluN2A C-terminal (rabbit, 1:800, Invitrogen A6473), phospho-Tyr1472-GluN2B (rabbit, 1:800, Phosphosolutions, p1516-1472), phospho-Tyr1336-GluN2B (rabbit, 1:800, Phosphosolutions p1516-1336), GluN1 N-terminal (guinea pig, 1:1000, Alomone AGP-046), GluN3A –Ct (rabbit, 1:1000, Millipore 07-356), PSD-95 (goat, 1:1500, Abcam ab12093), synaptophysin (mouse, 1:1000, Proteintech 60191-1-Ig), CaMKIIα (rabbit, 1:1000, Proteintech 20666-1-AP), TGN46 (rabbit, 1:1000, Proteintech AB10597396), GFAP (mouse, 1:1000, Thermofischer MA5-12023), EEA1 (mouse: 1:1000, Hybridoma Bank PCRP-EEA1-1F8) and finally

α-tubulin (1:4000, Sigma–Aldrich), as a loading control. Primary antibody binding was visualized with fluorescent secondary antibodies (IRDye, 1: 10000, Bonsay), and images were acquired using an Odyssey CLx Infrared Imaging system (LI-COR Biosciences GmbH).

2.5 | Immunoprecipitation assays

Brain extracts (100 μg in 500 μL phosphate buffered saline [PBS]) were incubated on a roller overnight at 4°C with Protein A Sepharose CL-4B (100 μL, Cytiva 17078001) coupled with antibodies against GluN2B N-terminal (rabbit, 15 μL, Alomone AGC-003), GluN2B N-terminal (mouse, 10 μL, NeuroMab 75-097 Clone N59/20), GluN2A N-terminal (mouse, 10 μL, Hybridoma Bank N327/95), or GluN1 N-terminal (mouse, 10 μL, Hybridoma Bank N308/48). The same number of beads without coupled antibody was used as a negative control. The input, bound, and unbound fractions were analyzed by Western blotting using antibodies against the GluN2B C-terminal (Invitrogen MA1-2014), GluN2A C-terminal (Invitrogen A6473) and GluN1 N-terminal (Alomone AGP-046).

2.6 | Enzymatic deglycosylation assays

Enzymatic deglycosylation was performed using an Agilent Enzymatic Deglycosylation Kit (Agilent Technologies, GK80110) following the manufacturer's instructions. Briefly, 100 μg of control or AD brain extract (SynF or ExsynF) was mixed with 10 μL incubation buffer and 2.5 μL denaturing buffer (both provided by the kit) and heated at 100°C for 5 min. Then, samples were cooled down to room temperature and 2.5 μL of detergent (15% w/v, NP-40) was added while mixing gently. Sialidase (1 μL), O-glycanase (1 μL), or N-glycanase (1 μL) enzymes were added to the samples and then heated at 37°C for 3 h.

2.7 | Lectin binding assays

SynF and ExsynF samples (50 μg) were incubated overnight at 4°C with lectins immobilized in agarose beads (100 μL), either Con A lectin (from *Canavalia ensiformis*; Sigma) or wheat germ agglutinin (WGA) lectin (from *Triticum vulgaris*, Sigma). After centrifugation at 3000×*g* for 1 min, the supernatant containing the unbound fraction was analyzed by Western blot. The proportion of unbound protein was calculated with respect to the total input.

2.8 | Statistical analysis

The distribution of data was tested for normality using a D'Agostino-Pearson test. Analysis of variance (ANOVA) was used for parametric variables and the Kruskal–Wallis test for non-parametric variables for comparison between groups. A Student's *t*-test for parametric variables and a Mann–Whitney *U* test for non-parametric variables were employed for comparison between two groups and for determining *p* values. For unpaired Student's *t*-test, a Welch's correction was employed in data with different standard deviations. Correlations were performed by Pearson correlation coefficients for parametric distributions and Spearman correlation coefficients for non-parametric distributions. The results are presented as the means ± SEM, and all the analyses were performed using GraphPad Prism (version 7; GraphPad Software, Inc). p-Value < 0.05 was considered significant.

3 | RESULTS

3.1 | SynF and ExsynF in human cortex

We have designed and validated an effective fractionation protocol to obtain synaptic and extrasynaptic membranes from frozen human cortex. This protocol is based on previous methods reported by other groups, designed for mouse fresh brains.[15,25] We have modified specific parameters such as Triton X-100 concentration, the use of acetone, and incubation times in key steps. In our protocol, cortical brain pieces were first homogenized as specified in Methods section and in Figure 1A, to obtain a supernatant that contained cell cytosol and microsomes (S2) and a P2 fraction of plasma membranes. P2 was incubated with 1% (w/v) Triton X-100 and centrifuged to get a supernatant fraction containing extrasynaptic membranes, which includes non-synaptic membranes and presynaptic membranes (extrasynaptic fraction, ExsynF); the pellet fraction was solubilized in RIPA buffer to collect post-synaptic membranes (synaptic fraction, SynF). Ultracentrifugation of S2 fraction was used to discriminate microsomal (P3) from cytosolic fractions (S3).

To validate this fractionation protocol in frontal cortices from controls and AD samples, synaptic and non-synaptic markers were assayed by Western blot (Figure 1B). PSD-95, a post-synaptic density protein, was mainly present in P2 and SynF, the fractions containing synaptic membranes. Synaptophysin, a presynaptic protein, was mainly observed in P2 and ExsynF, the fractions containing extrasynaptic membranes, but also at the cytosolic fraction (S2). The astrocytic glial fibrillary acidic protein (GFAP), a marker for glial cells, was mainly present at S2 and ExsynF. Non-synaptic-related proteins, as the early endosome-associated protein (EEA1) and the trans-Golgi network integral membrane protein 2 (detected with the TGN46 antibody) were enriched in S3 and P3 respectively, and not detected in SynF. Therefore, our protocol showed a high efficiency in discriminating cell compartments and specifically, synaptic and extrasynaptic membranes.

Since our goal was to characterize the synaptic and extrasynaptic distribution of NMDARs in the human cortex, it was compulsory to ensure the integrity and preservation of the *post mortem* samples prior to analysis. For this purpose, we estimated the HUman Synapse Proteome Integrity Ratio or "HUSPIR index",[26] which measures the ratio of proteolytic fragments of the NMDAR subunit GluN2B in SynF by immunoblots (Figure 1C). In human brain samples, particularly at synaptic membranes, GluN2B is present as a ~170 kDa full-length protein, but also detectable as ~150 and ~130 kDa species.

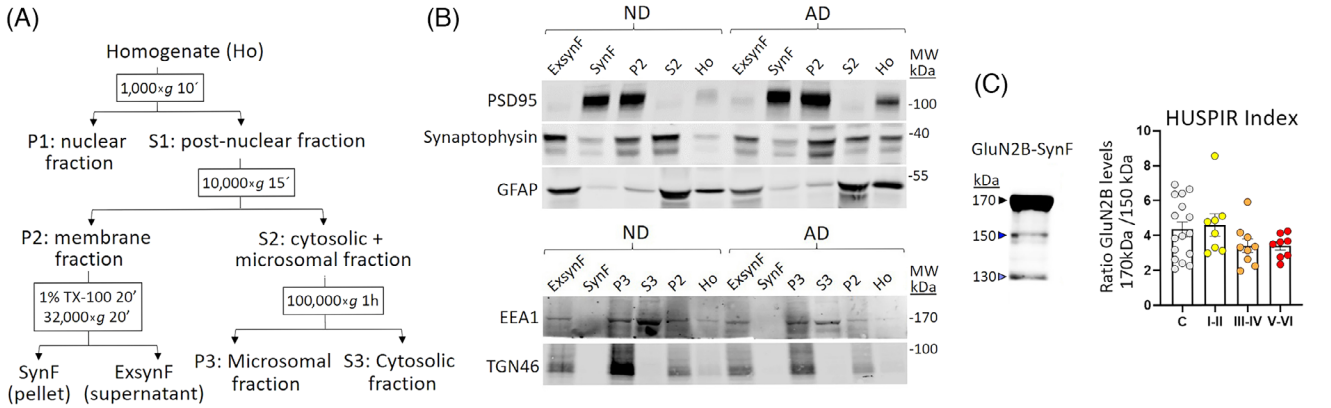

FIGURE 1 Validation of the fractionation protocol in human *post mortem* cortex. (A) Scheme of the fractionation procedure indicating the centrifugation steps and the fractions resulting from each one. P: pellet. S: supernatant. In brief, cortical homogenates (Ho) were centrifuged a 1000×*g* to obtain a nuclear-free supernatant (S1) and a pellet (P1) containing the nucleus. Centrifugation at 10,000×*g* of S1 resolved a supernatant that contained cell cytosol and microsomes (S2) and a pellet (P2) of plasma membranes. P2 was incubated with 1% (w/v) Triton X-100 and centrifuged at 32,000×*g* to obtain a supernatant fraction collected contained extrasynaptic membranes (ExsynF); the pellet fraction was solubilized in RIPA buffer to obtain the post-synaptic membranes (synaptic fraction, SynF). Ultracentrifugation at 100,000×*g* of S2 fraction served to obtain microsomal (P3) and cytosolic fractions (S3). (B). Western blot of different fractions from the fractionation protocol revealed with antibodies against synaptic-related proteins (PSD-95, synaptophysin), astroglial cells (glial fibrillary acidic protein [GFAP]) and no synaptic proteins associated to early endosome-associated protein (EEA1) and to Golgi apparatus (TGN46), in control and AD samples. (C) Representative Western blot of the N-methyl-D-aspartate receptor (NMDAR) subunit GluN2B, revealed with an antibody against the C-terminal of GluN2B, of a synaptic fraction from a control sample and the quantification of the HUSPIR index for all samples (controls $n = 16$, Braak I–II $n = 8$, Braak III–IV $n = 9$ and Braak V–VI $n = 8$).

These two shorter bands correspond to proteolytic fragments which increase during *post mortem* degradation.[27] A GluN2B full-length-170 kDa/fragment-150 kDa ratio, or HUSPIR index, above 1 indicates good synaptic structure integrity, which is more commonly found in *post mortem* cortical regions with respect to non-cortical regions.[26] The HUSPIR index of our brain cortical samples averaged 3.85 ± 1.5 (controls: 4.19 ± 0.4; AD: 3.65 ± 0.25, $p = 0.29$; no differences were found when comparing AD samples sub-grouped by Braak stages). This index indicates a high synaptic structural integrity and an optimal quality for biochemical analysis of our control and AD samples. Samples with a HUSPIR index ≤ 1 were removed from the study.

3.2 | SynF and ExsynF characterization of NMDAR subunits

The evaluation of NMDAR subunits distribution in SynF and ExsynF was performed by Western blot to make the discrimination of these two fractions possible. When equal amounts of SynF and ExsynF (10 μg) were loaded, it was clearly observed that NMDAR subunits were more abundant in synaptic membranes. To allow a quantitative analysis of fewer abundant extrasynaptic NMDAR subunits, we used a five times higher concentration (50 μg) of ExsynF in all subsequent Western blots.

We first characterized the expression of NMDAR subunits in brain cortices from controls in S2 (50 μg; containing the cytosol and therefore predictably low levels), P2 (10 μg), SynF (10 μg) and ExsynF (50 μg, Figure 2A). GluN2B and GluN2A full-length subunits were present at SynF with the expected ~170 kDa molecular mass. At ExsynF, GluN2B and GluN2A immunoreactivity showed an additional ~160 kDa band. GluN1 and GluN3 were observed as a 120 and 130 kDa bands respectively, both with the same apparent molecular mass in SynF and ExsynF. Remarkably, GluN3A seemed to be an exception with respect to the rest of NMDAR subunits, as it was more abundant at extrasynaptic membranes, as reported by other groups in mouse brain.[28,29] To confirm the identity of GluN2B, GluN2A, and GluN1, in SynF and ExsynF, we performed immunoprecipitations to pull down the NMDAR subunits, resolving with alternative antibodies that verified the identity of the bands (Figure 2B). To verify the identity of the GluN3A band we employed mice lacking GluN3A (*Grin3a*$^{-/-}$). The absence of the GluN3A-130 kDa band in *Grin3a*$^{-/-}$ brain extracts, but not in those from the wild-type, validated the identity of the GluN3A subunit (Figure 2C).

3.3 | Identification of GluN2B and GluN2A glycoforms

We aimed to understand why GluN2B and GluN2A subunits appeared as two distinct species in extrasynaptic membranes. NMDAR subunits are post-translationally modified by glycosylation, an adjustment key for their function and sorting.[10,30,31] Therefore, we hypothesized that extrasynaptic GluN2B-160 kDa and GluN2A-160 kDa could represent different glycoforms of the synaptic subunits. To test this, we performed an enzymatic deglycosylation assay in control and AD samples. Enzymatic deglycosylation (N-glycanase + syalidase + O-glycanase) of synaptic membranes induced a change in the electrophoretic mobility of GluN2A and GluN2B as a result of the removal of sugars.

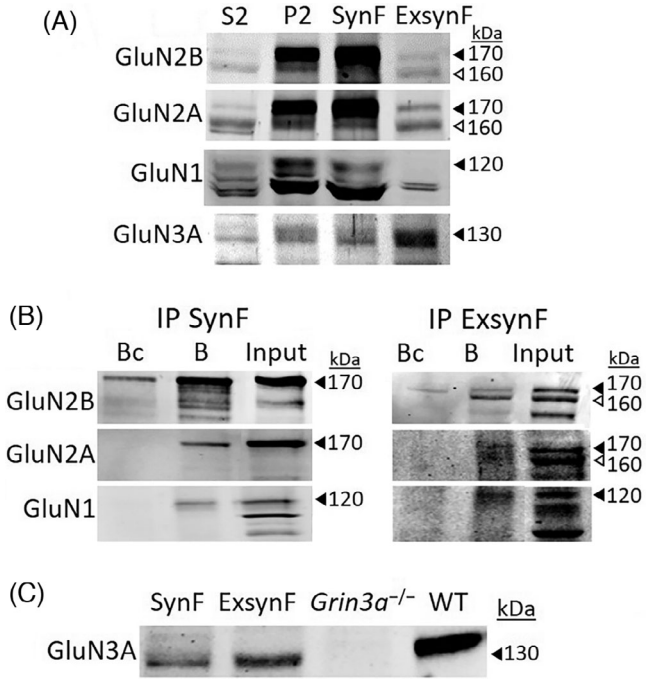

FIGURE 2 Characterization of N-methyl-D-aspartate receptor (NMDAR) subunits in SynF and ExsynF. (A) Representative blots of the NMDAR subunits GluN2B, GluN2A, GluN1, and GluN3A from different fractions of the fractionation protocol (50 μg for S2 and extrasynaptic membranes [ExsynF]; 10 μg for P2 and synaptic fraction [SynF]). Black arrowheads indicate bands corresponding to ~170 kDa GluN2B, ~170 kDa GluN2A, ~120 kDa GluN1 and ~130 kDa GluN3A in each blot. White arrowheads indicate ~160 kDa bands of GluN2B and GluN2A. (B) Immunoprecipitations (IP) of SynF and ExsynF of control samples. IP of GluN2B (antibody GluN2B N-terminal, rabbit, 10 μL, Alomone AGC-003); revealed with antibody against GluN2B C-terminal (mouse, 1:800, Invitrogen MA1-2014). IP of GluN2A (antibody GluN2A N-terminal, mouse, 100 μL supernatant, HybridomaBank N327/95) revealed with antibody against GluN2A C-terminal (rabbit, 1:800, Invitrogen A6473). IP of GluN1 (antibody GluN1 N-terminal, guinea pig, 10 μL, Alomone AGP-046) revealed with antibody against GluN1 N-terminal (mouse, 30 μL supernatant, HybridomaBank, N308/48). Bc, bound from control IP (IgG); B, bound fraction from the IP; Input, SynF or ExsynF. (C) Western blot of brain homogenates from a wild-type mouse (WT), a mouse lacking GluN3A (*Grin3a*$^{-/-}$) and from control human samples (SynF and ExsynF) revealed with GluN3A -Ct (rabbit, 1:1000, Millipore 07-356).

Remarkably, it was only in the presence of N-glycanase when the mobility of these subunits was affected, which suggests that their glycosylation was mainly due to N-glycosylation. In ExsynF, the N-deglycosylation simplified the 170 and 160 kDa bands of GluN2B and GluN2A to a single immunoreactive band, the 160 kDa band (Figure 3A). This indicated that GluN2B and GluN2A are expressed as two different glycoforms. The 170 kDa form would be predominantly found at synaptic membranes and correspond to fully glycosylated subunits, which are likely to be mature forms that harbor N-linked sugars. The 160 kDa glycoform would be almost exclusively at extrasynaptic membranes and could represent different glycoforms of synaptic GluN2B and GluN2A. When N-deglycosylation was performed in AD fractions, the NMDAR subunits exhibited similar migration change as in controls, in both SynF and ExsynF (Figure 3B).

3.4 | Tyr1336 is the main site for GluN2B phosphorylation

GluN2B-170 kDa phosphorylation at Tyr1472 and Tyr1336 was analyzed in SynF and ExsynF to evaluate whether there is a preferential phosphorylation site associated with each membrane fraction (Figure 4A). In SynF from control and AD cases (Braak stage V–VI), GluN2B was phosphorylated at Tyr1472 and Tyr1336, showing higher levels of the last. Interestingly, phosphorylation at Tyr1472 was identified only in synaptic membranes and was almost undetectable in extrasynaptic membranes (Figure 4B). This indicated that GluN2B is phosphorylated at Tyr1472 almost exclusively at synapses, while phosphorylation at Tyr1336 occurs in synaptic and extrasynaptic membranes.

3.5 | Synaptic and extrasynaptic distribution of NMDAR subunits in control and AD cortex

We next compared NMDAR subunit levels in control and AD cases sub-grouped by different Braak stages of neurodegeneration related to AD. Quantitative infra-red Western blotting has a greater linear range of detection than the more widely used chemiluminescent technique; however, due to the large differences in the levels of NMDAR subunits between membrane fractions, we analyzed P2, SynF, and ExsynF samples in separate blots to make the analysis feasible and more reproducible. We observed the same banding pattern in synaptic membranes and extrasynaptic membranes for all the NMDAR subunits when comparing control and AD samples (Figure 5A). Quantification (Figure 5B) revealed that P2 fractions expressed significantly lower levels of GluN2B in AD than control tissues when pooling all Braak stages (58.2 ± 37.0%; $p = 0.0009$) and in each independent stage, except for Braak III–IV, that showed a tendency to decrease (67.0 ± 25.6%; $p = 0.072$). Similarly, GluN2A levels were significantly lower in AD when pooling all Braak stages (57.2 ± 53.7%; $p = 0.0006$) and in Braak III–IV (56.1 ± 9.3%; $p = 0.020$). GluN1 levels were significantly lower in AD than in controls when taking all Braak stages into account (80.3 ± 25.2%; $p = 0.039$), and in Braak V–VI (69.36 ± 22.8%; $p = 0.041$). As previously reported,[32] GluN3A levels did not change between control and AD fractions. Since SynF contributes more to P2 signal than ExsynF, synaptic membrane levels of NMDAR subunits mirrored the decrease observed in P2. Both GluN2B and GluN2A levels were significantly lower in all Braak stages overall relative to controls (67.3 ± 43.0%, $p = 0.022$; 63.2 ± 44.5%, $p = 0.017$, respectively), and in Braak III–IV and V–VI stages for GluN2A (54.4 ± 33.4%, $p = 0.043$; 55.6 ± 34.9%, $p = 0.050$ respectively). GluN1 and GluN3A levels did not change in AD in overall or individual Braak stages relative to controls.

Interestingly, NMDAR subunit levels in extrasynaptic membranes displayed an opposite trend to those observed in synaptic

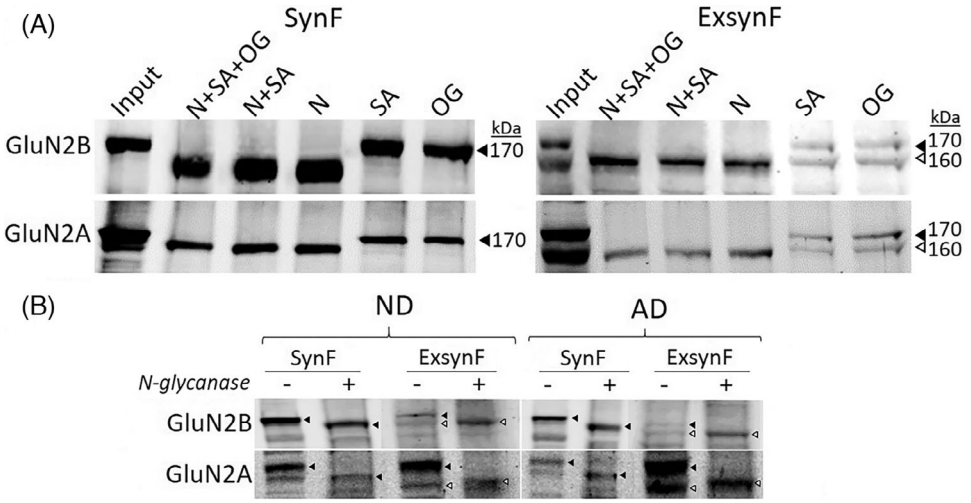

FIGURE 3 Glycosylation of N-methyl-D-aspartate receptor (NMDAR) subunits. (A) Enzymatic deglycosylation of synaptic fraction (SynF) and extrasynaptic membranes (ExsynF) (3B) with N-glycanase (N), syalidase (SA), O-glycanase (OG), or a combination of them in control samples, revealed with antibodies against Glun2B C-terminal (Invitrogen MA1-2014) and GluN2A C-terminal (Invitrogen A6473). Black arrowheads indicate bands corresponding to ~170 kDa GluN2B and ~170 kDa GluN2A. White arrowheads indicate ~160 kDa bands of GluN2B and GluN2A. (B) NMDAR subunits in SynF and ExsynF fractions from control and AD cases, after N-deglycosilation (+) or in unprocessed samples (-), revealed with antibodies against the C-terminal of GluN2B and GluN2A.

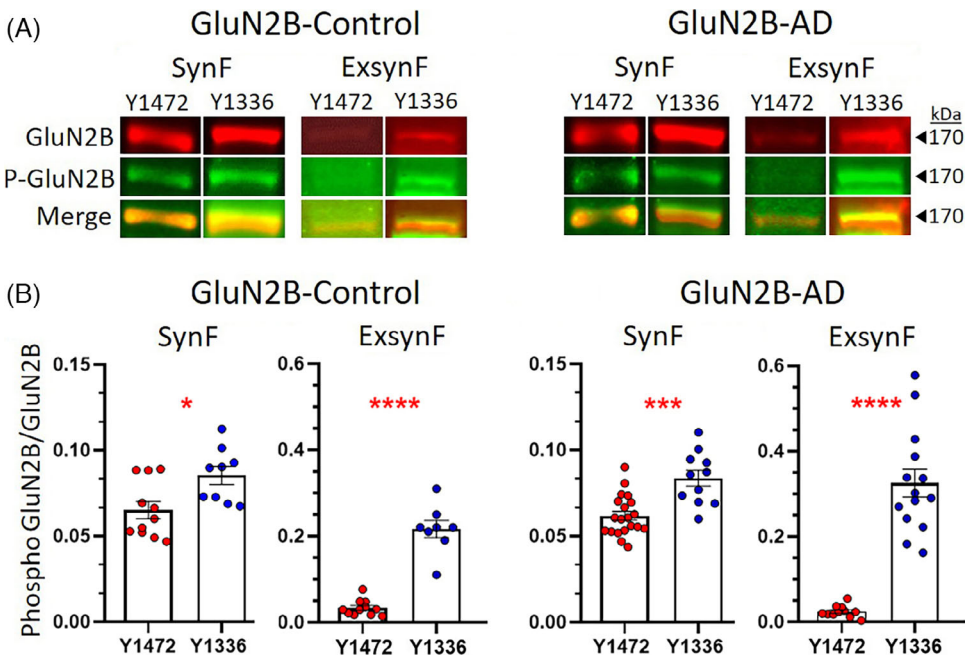

FIGURE 4 Comparison of GluN2B phosphorylation in synaptic fraction (SynF) and extrasynaptic membranes (ExsynF) between control and Alzheimer's disease (AD) cases. (A) Representative blots and (B) quantification of GluN2B (total protein resolved with mouse C-terminal antibody MA1-2014) and GluN2B phosphorylation (P-GluN2B) at Tyr1472 (rabbit antibody p1516-1472) and at Tyr1336 (rabbit antibody p1516-1336) in synaptic and extrasynaptic GluN2B-170 kDa from control and AD samples (Braak V–VI). The fluorescence of the secondary antibodies (IRDye 680RD goat anti-mouse, red; IRDye 800CW goat anti-rabbit, green) was detected with the Odyssey CLx Infrared Imaging system (LI-COR); merge fluorescence shows co-localization (yellow). Ratio of phosphorylated GluN2B respect to total GluN2B levels are plotted. Cases control SynF $n = 9–11$; control ExsynF $n = 8–11$; AD SynF $n = 11–20$; AD ExsynF $n = 11–14$. Observe the different Y scale for ExsynF graphs. $^{*}p < 0.05$, $^{**}p < 0.001$ with respect to control, *t*-test.

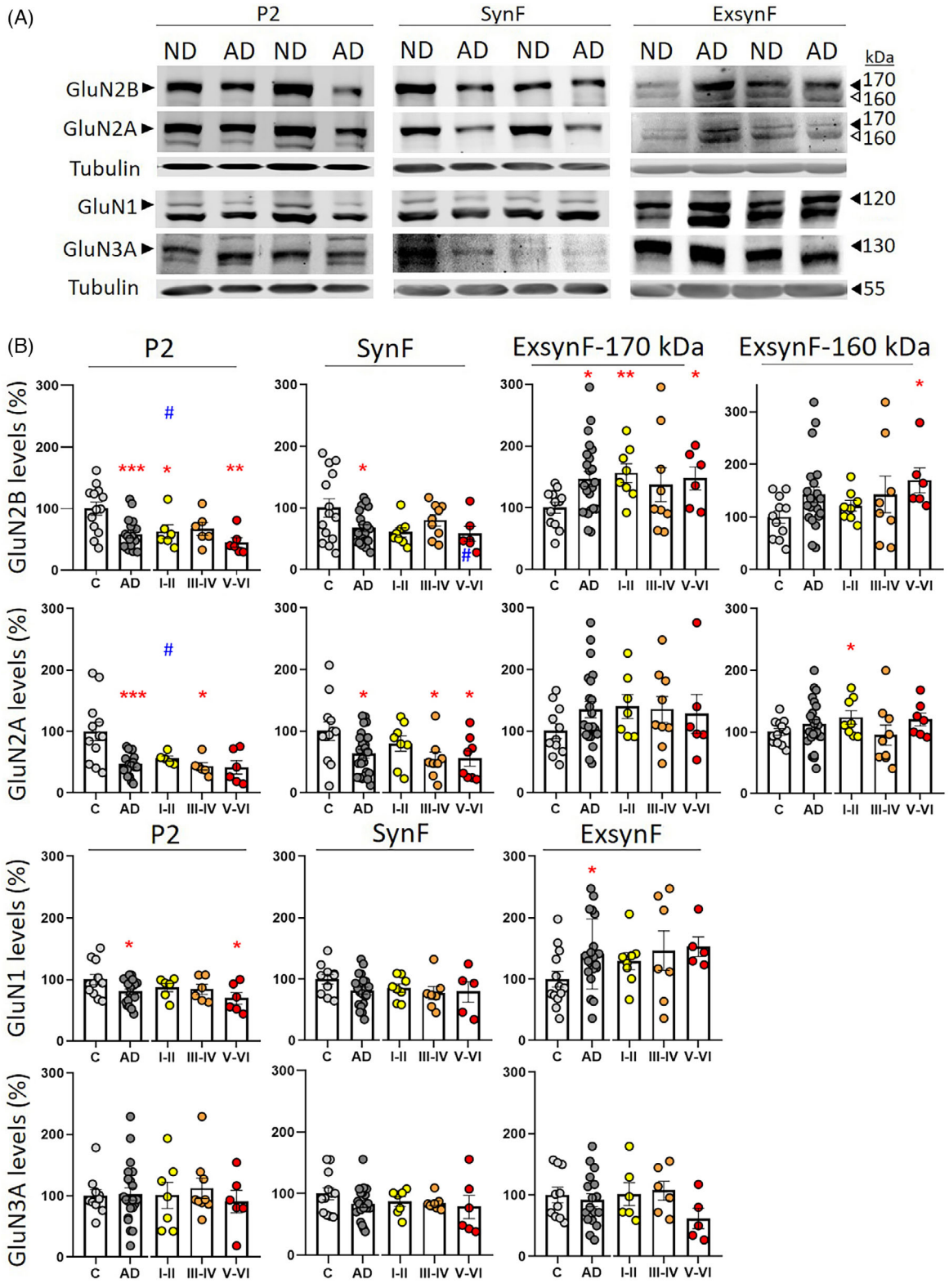

FIGURE 5 Distribution of N-methyl-D-aspartate receptor (NMDAR) subunits in membrane-containing fractions from control and Alzheimer's disease (AD) cases. (A) Representative Western blots of NMDAR subunits in membrane fraction (P2, 10 μg), synaptic fraction (SynF, 10 μg) and extrasynaptic fractions (ExsynF, 50 μg) from control and AD samples (Braak V–VI). Tubulin was used to normalize quantifications. (B) Quantification of NMDAR subunits levels at different Braak stages and all Braak stages together (AD: Braak stages I–VI) expressed as percentage respect to controls. GluN2B-170 kDa and GluN2A-170 kDa levels were measured in P2, SynF and ExsynF; GluN2B-160 kDa and GluN2A-160 kDa were measured in ExsynF only. $^{*}p < 0.05$, $^{**}p < 0.01$, $^{***}p < 0.001$ respect to control, *t*-test; $\#p < 0.01$ analysis of variance (ANOVA) one-way comparing control and all Braak stages. Cases control P2 $n = 10–13$; control SynF $n = 10–14$; control ExsynF $n = 10–12$; AD P2 $n = 18–22$; AD SynF $n = 21–24$; AD ExsynF AD $n = 17–24$.

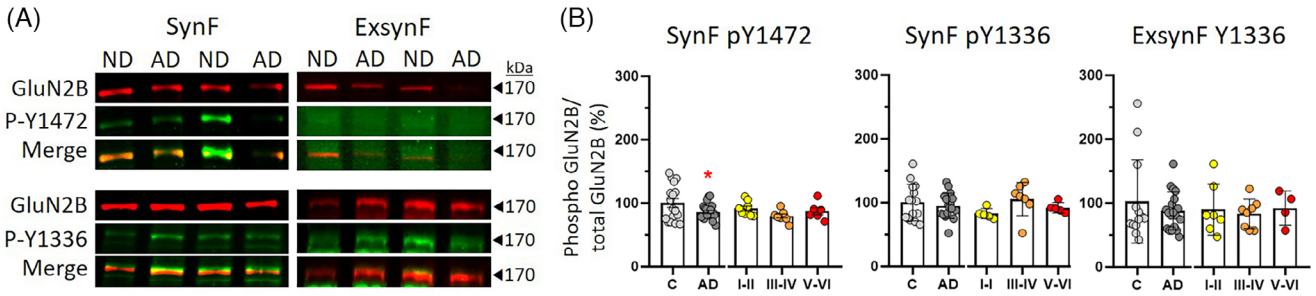

FIGURE 6 GluN2B phosphorylation from control and Alzheimer's disease (AD) cases comparing synaptic fraction (SynF) and extrasynaptic membranes (ExsynF). (A) Representative Western blots of GluN2B, phospho GluN2B Tyr1472, and phospho GluN2B Tyr1336 in SynF and ExsynF of controls and AD (Braak V–VI) samples. (B) Quantification of GluN2B-170 kDa phosphorylation at SynF (phospho Tyr1472, phospho Tyr1336) and at ExsynF (phospho Tyr1336). Levels of phosphorylated GluN2B were normalized to total GluN2B and estimated as in Figure 4. $^*p < 0.05$ AD *v* control, *t*-test. Cases control SynF $n = 15–17$; control ExsynF $n = 13$; AD SynF $n = 17–22$; AD ExsynF $n = 19$.

membranes, suggesting a subcellular redistribution in AD cases (Figure 5B). Extrasynaptic GluN2B-170 kDa levels were higher in AD overall (146.5 ± 55.6%; $p = 0.016$) and in most individual Braak stages compared to controls. Notably, the glycoform GluN2B-160 kDa displayed higher levels only at Braak V–VI (169.5 ± 58.0%; $p = 0.010$). Extrasynaptic GluN2A-170 kDa levels showed a tendency to be higher overall in AD than controls (134.8 ± 56.8%; $p = 0.098$), and the 160 kDa glycoform was significantly more abundant in Braak stages I–II compared with controls (123.5 ± 30.8%; $p = 0.050$), and a tendency in Braak stage V–VI (120.4 ± 27.7%; $p = 0.076$). Extrasynaptic GluN1 was significantly higher in overall AD (137.3 ± 49.9%; $p = 0.039$). Remarkably, GluN3A, the unique NMDAR subunit that is more abundant in ExsynF membranes than in SynF, did not show any change in ExsynF from AD tissues.

To confirm that changes in NMDAR subunits levels were related to the pathology of each group rather than to the age, we performed correlations in controls and at each Braak stage. No association between age and the levels of any NMDAR subunit was found in P2 and SynF in control or Braak stages. In ExsynF, a positive correlation was found in Braak V–VI for GluN2A ($p = 0.037$, *Pearson*) and GluN2B-160 kDa ($p = 0.008$, *Pearson*). This indicated that the higher levels of these subunits were found in the oldest subjects at the late stages of the pathology. In control ExsynF GluN2A-160 kDa and control and Braak I–II stage ExsynF Glun3A, levels correlated with age ($p = 0.0358$; positive correlation, *Pearson*; $p = 0.050$, negative correlation, *Pearson*; $p = 0.037$, negative correlation, respectively) although it did not seem to affect quantification (see Figure 5). We also analyzed the correlation between NMDAR subunit levels and the gender of the individuals, but no association was found in any group. There was no correlation between age and GluN2B phosphorylation at either Tyr1472 or Tyr1336 in any group.

3.6 | Low Tyr1472 phosphorylation at synaptic GluN2B in AD cortex

We then examined the phosphorylation pattern of GluN2B-170 kDa between controls and different Braak stages of AD (Figure 6A). The only significant difference was an overall lower GluN2B phosphorylation at Tyr1472 in SynF of AD tissue relative to controls (88.1 ± 15.3%; $p = 0.043$); phosphorylation at Tyr1336 remained unchanged. In ExsynF, no changes were observed between control and AD fractions in Tyr1336 phosphorylation (Figure 6B). Phosphorylation at Tyr1472 was too weak to be evaluated in ExsynF, as mentioned before. This finding suggests that the stabilization of GluN2B at synapses could be compromised in AD due to low levels of Tyr1472 phosphorylation.

3.7 | N-glycosylation is altered in extrasynaptic GluN2B and GluN2A in AD cortex

Modifications of N-glycosylation have been reported in AD for many glycoproteins; consequently, we evaluated whether the glycosylation of NMDAR subunits is affected. To this end, SynF and ExsynF from controls and AD samples (Braak V–VI) were incubated with lectins, which bind to specific carbohydrates linked to protein residues. We employed two agarose-immobilized lectins, Con A (binds mannose/glucose) and WGA (binds N-acetyl-D-glucosamine and sialic acid residues), that previously have demonstrated a saccharide-specificity and high affinity for NMDAR subunits.[31] After incubation, the levels of unbound glycoforms were determined by Western blot (Figure 7A) and quantified for each lectin. The unbound fractions of GluN2B-170 kDa and GluN2A-170 kDa were measured only in SynF, as the affinities of either Con A or WGA lectins for these subunits were so high in ExsynF that it made it difficult to quantify the unbound fraction, due to its weakness in the immunoblot. In SynF the percentages of GluN2B, GluN2A, and GluN1 unbound to lectins showed no differences among controls and AD (Figure 7B). Likewise, ExsynF GluN1 unbound fraction to ConA and WGA was similar in controls and AD. GluN3A affinity for Con A and WGA lectins was so high in SynF and ExsynF from both control and AD samples that the unbound fraction was quite weak; therefore, it was not quantified either. Statistical differences were found only in the ExsynF GluN2B-160 kDa and GluN2A-160 kDa, both with lower unbound percentages to Con A in AD fractions with respect to controls, indicating a higher affinity for this lectin. This suggests a specific AD-related alteration in the glycosylation of these extrasynaptic GluN2B and GluN2A glycoforms.

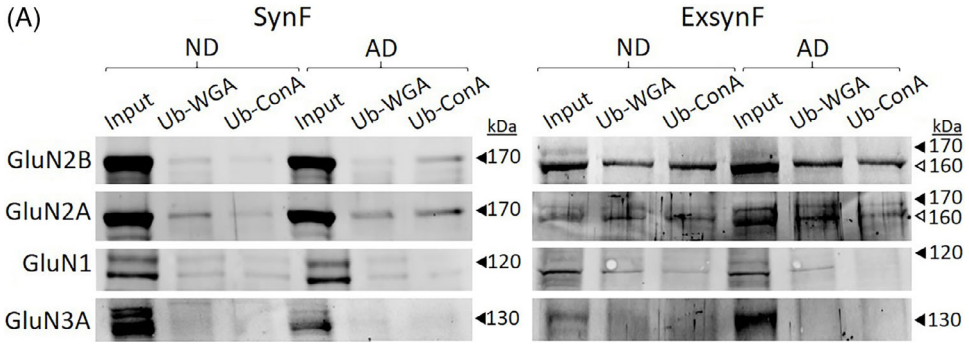

(B)

		WGA		ConA	
		C	AD	C	AD
SynF	GluN2B-170	3.0 ± 3.0	2.2 ± 1.8	2.2 ± 2.5	3.9 ± 3.4
	GluN2A-170	5.9 ± 2.6	4.3 ± 2.7	4.9 ± 3.4	4.8 ± 3.1
	GluN1	18.8 ± 10.4	8.6 ± 6.1	11.7 ± 7.4	6.1 ± 6.1
	GluN3A	*n.d.*	*n.d.*	*n.d.*	*n.d.*
ExsynF	GluN2B-160	56.6 ± 18.1	55.8 ± 22.6	76.7 ± 29.0	54.2 ± 36.4 *
	GluN2A-160	62.7 ± 30.3	51.0 ± 27.0	83.0 ± 24.9	52.6 ± 40.4 *
	GluN1	53.4 ± 40.3	34.8 ± 4.5	34.2 ± 31.4	17.2 ± 13.3
	GluN3A	*n.d.*	*n.d.*	*n.d.*	*n.d.*

FIGURE 7 N-Methyl-D-aspartate receptor (NMDAR) subunits interaction with N-glycan lectins. (A) Representative Western blots for GluN2B, GluN2A, GluN1, and GluN3A of unbounds and inputs of synaptic fraction (SynF) and extrasynaptic membranes (ExsynF) fractions after incubation with wheat germ agglutinin (WGA) and Con A lectins, from control and Braak stage V–VI samples. (B) Quantification of SynF and ExsynF unbound fraction to WGA or Con A lectins from control and AD samples, with respect to the input fraction (SynF or ExsynF respectively) expressed as percentage (%). Data represent SynF GluN2B-170 kDa, SynF GluN2A-170 kDa, SynF GluN1, ExsynF GluN2B-160 kDa, ExsynF GluN2A-160 kDa, and ExsynF GluN1. Values represent percentage unbound ± standard deviation. Control SynF $n = 5$, controls ExsynF $n = 7$; Braak V–VI SynF $n = 6$, Braak V–VI ExsynF $n = 7$. *nd*, not determined.

3.8 | NMDAR subunits distribution in mice models

Finally, we used two mouse models to determine whether dysfunction in AD key proteins, tau and APP, could be related to changes in NMDAR subunits distribution among synaptic and extrasynaptic membranes. The same fractionation protocol was used, yielding a high discrimination among cytosolic, synaptic, and extrasynaptic fractions (Figure 8A). In all immunoblots, mouse NMDAR subunits were identified at similar molecular mass than in human samples, but ExsynF GluN2B and GluN2A were resolved as a unique band. The first transgenic line used, TauP301S is a tauopathy model that expresses the human P301S mutant tau protein and is characterized by neurofibrillary pathology and neurological manifestations.[33] At 9 months of age, a decrease was observed in SynF GluN2B (62.3 ± 27.6%; $p = 0.009$), SynF GluN1 (62.2 ± 27.6%; $p = 0.009$), and ExsynF GluN3A levels (62.2 ± 31.3%; $p = 0.014$) when compared with those in wild-type mice (Figure 8B, C). This resembles somehow what occurs in AD samples and suggests that tau phosphorylation could be involved in GluN2B/GluN1 and GluN3A/GluN1 retention at their main synaptic locations. A second transgenic model, the APP/PS1 mouse,[34] develops amyloid plaques pathology, astrogliosis, and learning deficits starting at 7 months of age.[35,36] In this model, at 12 months of age only GluN1 levels were affected, in both SynF (33.2 ± 4.3%; $p = 0.0317$) and ExsynF (57.3 ± 24.6%; $p = 0.003$), compared with wild-type controls (Figure 8B, D). In any of these mouse models, phosphorylation of GluN2B was affected, suggesting that Fyn kinase activity may not been altered in these transgenic mice.

4 | DISCUSSION

For the first time, we have described the distribution of the main four NMDAR subunits -GluN2B, GluN2A, GluN1, and GluN3A- between synaptic and extrasynaptic membranes in the human cortex. The different nature of these membranes makes it possible to use biochemical fractionation protocols and separate synaptic membranes, defined as plasma membrane of the post-synaptic density, and extrasynaptic membranes, which include spine necks, dendritic shafts, or somas, which are further away from the post-synaptic density.[37,38] We have characterized the distribution of NMDAR subunits, as well as the phosphorylation, and glycosylation levels in membrane fractions from controls and AD subjects.

We have found that in the human brain, GluN2B, GluN2A, and GluN1 subunits are enriched in synaptic membranes, while GluN3A predominates in extrasynaptic membranes, as previously reported in mouse brains due to lower stabilization at synaptic sites.[39] Early reports established that GluN2B-containing NMDAR is mainly extrasynaptic, while GluN2A-containing NMDAR is mainly synaptic.[4,40,41] This

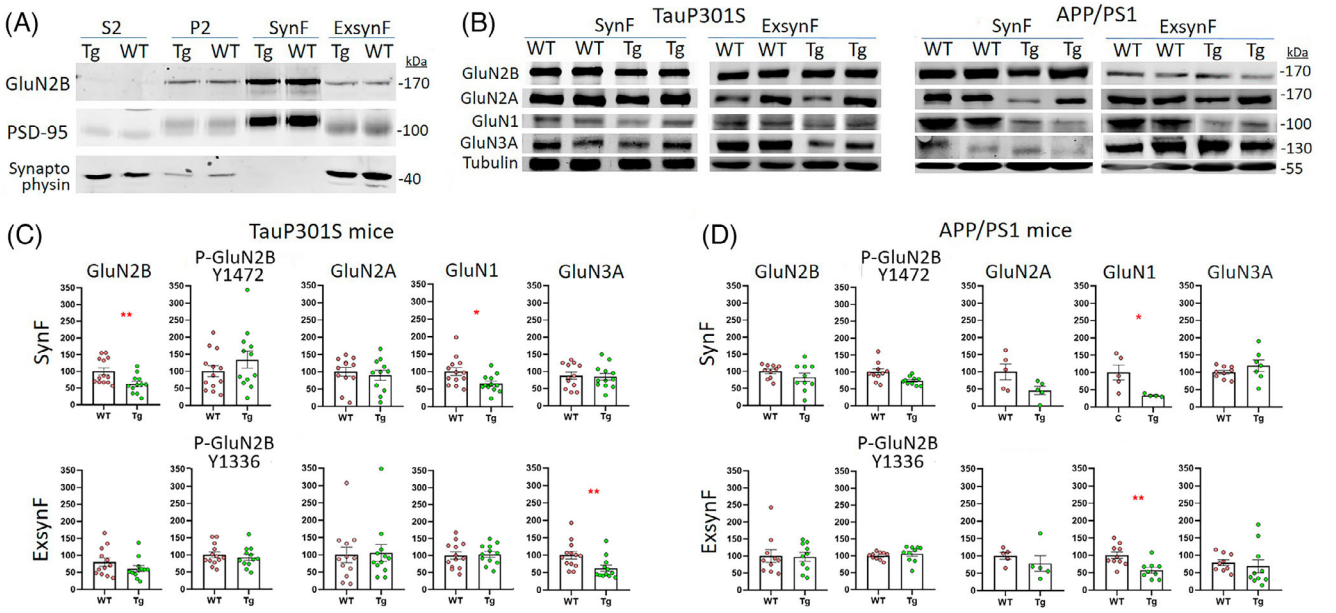

FIGURE 8 N-Methyl-D-aspartate receptor (NMDAR) subunit levels and GluN2B phosphorylation in Alzheimer's disease (AD) mouse models TauP301S and APP/PS1. (A) The fractionation protocol in wild-type mice (WT) and transgenic mice (Tg) cortex was the same as that described for human samples in Figure 1. Representative Western blot of S2, P2, synaptic fraction (SynF), and extrasynaptic membranes (ExsynF) fractions from WT and TauP301S mice (Tg) developed with antibodies against Glun2B, post-synaptic density95 (PSD95), synaptophysin, and glial fibrillary astrocytic protein (GFAP); similar patterns were obtained for APP/PS1 mice (not shown). (B) Representative Western blots of NMDAR subunits in SynF and ExsynF from WT and TauP301S mice (Tg); and from WT and APP/PS1 mice (Tg), as indicated. (C) Quantification of GluN2B, Tyr1472 phosphorylation of GluN2B (P-GluN2B Tyr1472), Tyr1336 phosphorylation of GluN2B (P-GluN2B Tyr1472), GluN2A, GluN1, and GluN3A levels in SynF and ExsynF from WT and TauP301S mice (Tg). WT SynF $n = 6–13$, WT ExsynF $n = 12–13$, Tg SynF $n = 6–12$, Tg ExsynF $nn = 12$. (D) Quantification of GluN2B, Tyr1472 phosphorylation of GluN2B (P-GluN2B Tyr1472), Tyr1336 phosphorylation of GluN2B (P-GluN2B Tyr1472), GluN2A, GluN1, and GluN3A levels in SynF and ExsynF from WT and APP/PS1 mice (Tg). WT SynF $n = 5–10$, WT ExsynF $n = 5–10$, Tg SynF $n = 5–10$; Tg ExsynF $n = 5–10$. $^{**}p < 0.01$ respect to WT.

led to the notion that extrasynaptic GluN2B-containing NMDAR drives long-term depression and excitotoxicity, while GluN2A-containing NMDAR mediates for long-term potentiation (LTP) and survival cell signaling.[42] However, this oversimplified idea was challenged by studies that found that GluN2B and GluN2A subunits are present in both synaptic and extrasynaptic membranes.[43] Furthermore, activation of synaptic and extrasynaptic NMDARs is equally capable of inducing excitotoxicity,[44] and synaptic GluN2A-containing NMDAR is also necessary to induce excitotoxicity.[45] Results may have differed along the studies because of different protocol conditions and lack of pharmacological/biochemical tools to definitively distinguish NMDAR subtypes; additionally, the employment of different neurodevelopmental stages in mice can also contribute to discrepancies in the interpretations.[46]

Despite discrepancies, an imbalance between synaptic and extrasynaptic NMDAR activity has been considered as a possible pathogenic factor for neurodegenerative diseases, and a major contributing factor to glutamatergic dysfunction and pathogenesis in AD.[46,47] Our approach to study NMDAR subunits distribution in synaptic and extrasynaptic membranes, while not feasible using crude membrane preparations, uncovered relevant differences between controls and AD, particularly for GluN2B, and at specific neurodegenerative stages related to AD.

At synaptic membranes, the levels of the canonical GluN2B-170 kDa subunit were significantly lower in AD fractions compared with controls; but higher at extrasynaptic membranes. Similarly, the canonical GluN2A-170 kDa was less abundant in AD synaptic membranes and showed a tendency to increase in extrasynaptic membranes. GluN1 levels were similar at synaptic membranes in controls and AD, but at extrasynaptic membranes, levels were higher in AD. As an exception, GluN3A levels were unchanged in AD. In sum, we find an impaired distribution of NMDAR subunits levels between synaptic and extrasynaptic membranes in AD relative to control frontal cortex. The shift of NMDARs toward extrasynaptic membranes could be relevant to the excitotoxicity that is thought to be mediated by extrasynaptic NMDARs. Chronic NMDAR stimulation lasting for months to years has been associated with AD with increased levels of extrasynaptic GluN2B-containing NMDARs, which induce enlarged tonic NMDAR currents and excitotoxicity.[48,49] Remarkably, we have found higher levels of the canonical GluN2B-170 kDa and also of the GluN2B -160 kDa glycoform in Braak V–VI in extrasynaptic membranes. This suggests that excitotoxicity could be facilitated at the late stages of AD by GluN2B enrichment in extrasynaptic membranes.

Differences in NMDAR subunits expression have been observed in AD with respect to the control at different regions of the *post mortem* human cortex. Transcriptomic analysis has revealed that the

expression of GluN1 gene, *GRIN1*, is the most affected in the AD brain. *GRIN1* is downregulated in the temporal cortex and superior temporal gyrus[50,51] from AD individuals. Interestingly, in the prefrontal cortex *GRIN1* expression is modulated through AD progression, being upregulated at early-AD pathology with respect to control, and downregulated at late-AD pathology regarding early-AD pathology.[52] Other studies have not found changes in *GRIN1* expression in the frontal and prefrontal cortex,[50,53] or when transcriptomic analysis is performed in astrocytes.[54] Overall, these studies suggest that the low GluN1 protein levels observed in AD extrasynaptic membranes could be attributed to downregulation of *GRIN1* expression. Moreover, some studies report downregulation of *GRIN2B* and *GRIN2A* mRNA and protein levels in the hippocampus, and in the temporal entorhinal cortex from AD individuals.[51,55–58] In our study, GluN2B and GluN2A protein levels were lower in AD synaptic membranes and higher in extrasynaptic membranes. This suggests that the more dynamic transcriptional modifications, a key factor in regulating trafficking and sorting of these subunits to the membrane, would be responsible for the altered GluN2B and GluN2A distribution in AD, rather than due to transcriptional changes.

Deglycosylation and lectin binding analysis confirmed that GluN2B, GluN2A, GluN1, and GluN3A are glycosylated in human cortices, and indicated that GluN2B and GluN2A are N-glycosylated. N-Glycosylation is a complex process that involves numerous enzymes. It is a highly regulated mechanism that includes many sequential steps controlled by the ordered actions of a variety of glycosyltransferases, glycosidases, and other regulators in the endoplasmic reticulum and Golgi compartments.[59] It is not known which glucosyltransferases participate in GluN2A/B glycosylation; however, glycosylation is essential for NMDAR-dependent electric currents[30,60] and correct intracellular sorting. Glycosylation of AsnN675 in GluN2B has been identified as a requirement for trafficking NMDARs to synapses in an activity-independent manner.[61]

Remarkably, glycoforms of GluN2B and GluN2A with a lower apparent molecular mass (GluN2B-160 kDa and GluN2A-160 kDa) are found exclusively at extrasynaptic membranes in control and AD cases. Changes in protein glycosylation have been reported in AD,[62] even in N-linked glycosylation,[63] and in specific NMDAR subunits such as GluN2B, GluN2A, and GluN1.[64] Our lectin binding analysis demonstrated differences in extrasynaptic GluN2B-160 kDa and GluN2A-160 kDa glycoforms between controls and AD, with higher levels at Braak V–VI than in controls. This could be explained because N-glycosylation is a post-translational modification essential for NMDAR subunit surface delivery,[10] and altered glycosylation could affect the surface expression[65] and intracellular sorting[66] of GluN2B and GluN2A subunits. This would lead to increased levels at the extrasynaptic membranes of these glycoforms, rather than reflecting enhanced translocation from synaptic membranes.

We have previously described aberrant glycosylation in AD-related proteins, such as APP,[67] apoE,[68] reelin,[69] and acetylcholinesterase,[70] as well as changes in glycosylated epitopes.[71] Glycosylation changes in NMDAR subunits could occur early or be associated with neurodegeneration progression in AD, but whether the 160-kDa glycoforms of GluN2B and GluN2A modify NMDAR activity in AD should be determined.

In this study, GluN2B phosphorylation at Tyr1336 was significantly high in extrasynaptic membranes compared to Tyr1472 phosphorylation. At synaptic membranes, phosphorylation at Tyr1336 and Tyr1472 were quantifiable, but at extrasynaptic membranes phosphorylation at Tyr1472 was particularly low, making quantification difficult in both controls and AD fractions. Tyr1336 GluN2B phosphorylation levels showed consistency in control and AD fractions, which means that, independently of the different relative GluN2B levels in synaptic and extrasynaptic membranes from control and AD samples, the phosphorylation ratio at Tyr1336 remained similar in both conditions. On the contrary, phosphorylation levels of GluN2B at Tyr1472 relative to GluN2B levels were significantly low in AD synaptic membranes; and this suggests a non-proportional decay of phosphorylation of GluN2B with respect to the lower GluN2B levels found in AD and, therefore, a specific affectation of synaptic GluN2B Tyr1472 phosphorylation in AD.

It is broadly assumed that Tyr1472 is the major phosphorylation site within GluN2B.[72] GluN2B Tyr1472 phosphorylation activates and stabilizes NMDAR in synaptic plasma membrane, which prevents it from being endocytosed or translocated to non-clustered extrasynaptic membranes, and increases after LTP.[7,72] Our results suggest that the lesser synaptic Tyr1472 phosphorylation in AD could impair GluN2B retention at synaptic membranes, therefore explaining the higher levels at the extrasynaptic membranes. However, the proportion of the Tyr1472 GluN2B translocated was not sufficient to be measurable, and Tyr1336 GluN2B was the principal subunit in ExsynF. Our study raises questions about the role of synaptic GluN2B Tyr1336 phosphorylation, which is thought to promote NMDAR anchoring at extrasynaptic membranes,[14–16] as also indicated by our findings.

Glycosylation and phosphorylation are processes mostly studied separately; therefore, the relation between them is not fully understood. Specific interrelations have been suggested for key AD proteins such as APP[66] and tau.[73] However, the mechanistic relationship between glycosylation and phosphorylation on GluN2B mislocalization remains to be explored.

Our analysis of tau and Aβ transgenic models only partially reproduced the alterations found in AD patients, suggesting that some of the changes in NMDAR subunits observed in human AD brains are likely to be the consequence of complex or compensatory processes that could require the participation of more than one pathological alteration. However, studies using tau-based mouse models point in the same direction as our data. A shift in the balance from synaptic toward extrasynaptic NMDARs was described in the hippocampus of TauP301S mice at 10 months of age,[74] and tau knockout mice do not exhibit changes in NMDAR phosphorylation at Tyr1472 and Tyr1336,[16] suggesting that tau is not related to NMDAR phosphorylation, in agreement with our results. Therefore, the accumulation of phosphorylated tau is relevant to alter NMDAR distribution, but tau may not have a role in NMDAR phosphorylation. Furthermore, the amyloid peptide accumulation that occurs in APP/PS1 mice seems to affect only GluN1 in the frontal cortex, in agreement with

transcriptomic studies in the *post mortem* human brain.[50–52] However, studies in the hippocampus report low levels of GluN2B and GluN2A, and no changes in GluN1,[75] but also higher levels of GluN2B and phosphorylated GluN2B-Tyr1472 in the extrasynaptic fraction from hippocampal homogenates.[76] Our results suggest that, in the frontal cortex from APP/PS1 mice, reduced levels of the obligatory subunit GluN1 in synaptic and extrasynaptic membranes may affect all NMDARs, and contribute to the synaptic failure described in this model[77] driven by amyloid-beta.

In conclusion, the alterations in the NMDAR subunits distribution described here could affect essential NMDAR functions involved in processes such as synaptic plasticity and memory.[7,78,79] Consequently, the aforementioned alterations may contribute to the cognitive decline associated with normal aging and AD.[80] The shift to extrasynaptic membranes of GluN2B, GluN2A and GluN1, could explain the exacerbated NMDA-related excitotoxicity observed in AD.

ACKNOWLEDGMENTS

We particularly want to acknowledge patients and Biobank HUB-ICO-IDIBELL (PT20/00171) integrated in the ISCIII Biobanks and Biomodels Platform and Xarxa Banc de Tumors de Catalunya (XBTC) for their collaboration. This work was supported by grants from the Fondo de Investigaciones Sanitarias (PI22/01329, co-funded by the Fondo Europeo de Desarrollo Regional, FEDER "Investing in your future"), CIBERNED (Instituto de Salud Carlos III, Spain), and from the Direcció General de Ciència i Investigació, Generalitat Valenciana (AICO/2021/308). Sergio Escamilla is supported by a PFIS fellowship from the ISC-III, Centro de Excelencia Severo Ochoa, Agencia Estatal de Investigación (CEX2021-001165-S), Instituto de Investigación Sanitaria y Biomédica de Alicante (Isabial), and Programa Investigo, Conselleria de Innovación, Universidades, Investigación y Sociedad Digital, Generalitat Valenciana (INVEST-2023-157).

CONFLICT OF INTEREST STATEMENT

The authors declare no conflicts of interest. Author disclosures are available in the Supporting information.

CONSENT STATEMENT

Consent was not necessary.

ORCID

Inmaculada Cuchillo-Ibáñez https://orcid.org/0000-0002-3689-5518

REFERENCES

1. Paoletti P, Bellone C, Zhou Q. NMDA receptor subunit diversity: impact on receptor properties, synaptic plasticity and disease. *Nat Rev Neurosci*. 2013;14(6):383-400. doi:10.1038/NRN3504
2. Reisberg B, Doody R, Stöffler A, Schmitt F, Ferris S, Möbius HJ. Memantine in moderate-to-severe Alzheimer's disease. *N Engl J Med*. 2003;348(14):1333-1341. doi:10.1056/NEJMOA013128
3. Paoletti P. Molecular basis of NMDA receptor functional diversity. *Eur J Neurosci*. 2011;33(8):1351-1365. doi:10.1111/J.1460-9568.2011.07628.X
4. Sanz-Clemente A, Nicoll RA, Roche KW. Diversity in NMDA receptor composition: many regulators, many consequences. *Neuroscientist*. 2013;19(1):62-75. doi:10.1177/1073858411435129
5. Pegasiou CM, Zolnourian A, Gomez-Nicola D, et al. Age-dependent changes in synaptic NMDA receptor composition in adult human cortical neurons. *Cereb Cortex*. 2020;30(7):4246-4256. doi:10.1093/CERCOR/BHAA052
6. Wang R, Reddy PH. Role of glutamate and NMDA receptors in Alzheimer's disease. *J Alzheimers Dis*. 2017;57(4):1041-1048. doi:10.3233/JAD-160763
7. Prybylowski K, Chang K, Sans N, Kan L, Vicini S, Wenthold RJ. The synaptic localization of NR2B-containing NMDA receptors is controlled by interactions with PDZ proteins and AP-2. *Neuron*. 2005;47(6):845-857. doi:10.1016/J.NEURON.2005.08.016
8. Herz J, Chen Y. Reelin, lipoprotein receptors and synaptic plasticity. *Nat Rev Neurosci*. 2006;7(11):850-859. doi:10.1038/nrn2009
9. Cuchillo-Ibañez I, Balmaceda V, Mata-Balaguer T, Lopez-Font I, Sáez-Valero J. Reelin in Alzheimer's disease, increased levels but impaired signaling: when more is less. *J Alzheimer's Dis*. 2016;52(2):403-416. doi:10.3233/JAD-151193
10. Horak M, Barackova P, Langore E, Netolicky J, Rivas-Ramirez P, Rehakova K. The extracellular domains of GluN subunits play an essential role in processing NMDA receptors in the ER. *Front Neurosci*. 2021;15:603715. doi:10.3389/FNINS.2021.603715
11. Trepanier CH, Jackson MF, MacDonald JF. Regulation of NMDA receptors by the tyrosine kinase Fyn. *FEBS J*. 2012;279(1):12-19. doi:10.1111/J.1742-4658.2011.08391.X
12. Tezuka T, Umemori H, Akiyama T, Nakanishi S, Yamamoto T. PSD-95 promotes Fyn-mediated tyrosine phosphorylation of the N-methyl-D-aspartate receptor subunit NR2A. *Proc Natl Acad Sci U S A*. 1999;96(2):435-440. doi:10.1073/PNAS.96.2.435
13. Groveman BR, Feng S, Fang XQ, et al. The regulation of N-methyl- d -aspartate receptors by Src kinase. *FEBS J*. 2012;279(1):20-28. doi:10.1111/j.1742-4658.2011.08413.x
14. Hardingham GE, Fukunaga Y, Bading H. Extrasynaptic NMDARs oppose synaptic NMDARs by triggering CREB shut-off and cell death pathways. *Nat Neurosci*. 2002;5(5):405-414. doi:10.1038/nn835
15. Goebel-Goody SM, Davies KD, Alvestad Linger RM, Freund RK, Browning MD. Phospho-regulation of synaptic and extrasynaptic N-methyl-d-aspartate receptors in adult hippocampal slices. *Neuroscience*. 2009;158(4):1446-1459. doi:10.1016/j.neuroscience.2008.11.006
16. Pallas-Bazarra N, Draffin J, Cuadros R, Antonio Esteban J, Avila J. Tau is required for the function of extrasynaptic NMDA receptors. *Sci Rep*. 2019;9(1):9116. doi:10.1038/s41598-019-45547-8
17. Marco S, Giralt A, Petrovic MM, et al. Suppressing aberrant GluN3A expression rescues synaptic and behavioral impairments in Huntington's disease models. *Nat Med*. 2013;19(8):1030-1038. doi:10.1038/NM.3246
18. Yan J, Peter Bengtson C, Buchthal B, Hagenston AM, Bading H. Coupling of NMDA receptors and TRPM4 guides discovery of unconventional neuroprotectants. *Science*. 2020;370(6513):eaay3302. doi:10.1126/SCIENCE.AAY3302
19. Yu SP, Jiang MQ, Shim SS, Pourkhodadad S, Wei L. Extrasynaptic NMDA receptors in acute and chronic excitotoxicity: implications for preventive treatments of ischemic stroke and late-onset Alzheimer's disease. *Mol Neurodegener*. 2023;18(1):43. doi:10.1186/S13024-023-00636-1
20. Italia M, Ferrari E, Diluca M, Gardoni F. NMDA and AMPA receptors at synapses: novel targets for tau and α-synuclein proteinopathies. *Biomedicines*. 2022;10(7):1550. doi:10.3390/BIOMEDICINES10071550
21. Roselli F, Tirard M, Lu J, et al. Soluble beta-amyloid1-40 induces NMDA-dependent degradation of postsynaptic density-95 at

glutamatergic synapses. *J Neurosci*. 2005;25(48):11061-11070. doi:10.1523/JNEUROSCI.3034-05.2005
22. Chang L, Zhang Y, Liu J, et al. Differential regulation of N-methyl-D-aspartate receptor subunits is an early event in the actions of soluble amyloid-β(1-40) oligomers on hippocampal neurons. *J Alzheimers Dis*. 2016;51(1):197-212. doi:10.3233/JAD-150942
23. Li Y, Chang L, Song Y, et al. Astrocytic GluN2A and GluN2B oppose the synaptotoxic effects of amyloid-β1-40 in hippocampal cells. *J Alzheimers Dis*. 2016;54(1):135-148. doi:10.3233/JAD-160297
24. Braak H, Alafuzoff I, Arzberger T, Kretzschmar H, Del Tredici K. Staging of Alzheimer disease-associated neurofibrillary pathology using paraffin sections and immunocytochemistry. *Acta Neuropathol*. 2006;112(4):389-404. doi:10.1007/s00401-006-0127-z
25. Jiang X, Knox R, Pathipati P, Ferriero D. Developmental localization of NMDA receptors, Src and MAP kinases in mouse brain. *Neurosci Lett*. 2011;503(3):215-219. doi:10.1016/j.neulet.2011.08.039
26. Bayés À, Collins MO, Galtrey CM, et al. Human post-mortem synapse proteome integrity screening for proteomic studies of postsynaptic complexes. *Mol Brain*. 2014;7(1):88. doi:10.1186/S13041-014-0088-4
27. Wang Y, TesFaye E, Yasuda RP, Mash DC, Armstrong DM, Wolfe BB. Effects of post-mortem delay on subunits of ionotropic glutamate receptors in human brain. *Mol Brain Res*. 2000;80(2):123-131. doi:10.1016/S0169-328X(00)00111-X
28. Pérez-Otaño I, Luján R, Tavalin SJ, et al. Endocytosis and synaptic removal of NR3A-containing NMDA receptors by PACSIN1/syndapin1. *Nat Neurosci*. 2006;9(5):611-621. doi:10.1038/nn1680
29. Wee KSL, Tan FCK, Cheong YP, Khanna S, Low CM. Ontogenic profile and synaptic distribution of GluN3 proteins in the rat brain and hippocampal neurons. *Neurochem Res*. 2016;41(1-2):290-297. doi:10.1007/S11064-015-1794-8
30. Lichnerova K, Kaniakova M, Park SP, et al. Two N-glycosylation sites in the GluN1 subunit are essential for releasing N-methyl-d-aspartate (NMDA) receptors from the endoplasmic reticulum. *J Biol Chem*. 2015;290(30):18379-18390. doi:10.1074/JBC.M115.656546
31. Kaniakova M, Lichnerova K, Skrenkova K, Vyklicky L, Horak M. Biochemical and electrophysiological characterization of N-glycans on NMDA receptor subunits. *J Neurochem*. 2016;138(4):546-556. doi:10.1111/JNC.13679
32. Verhaeghe R, Elía-Zudaire O, Escamilla S, Sáez-Valero J, Pérez-Otaño I. No evidence for cognitive decline or neurodegeneration in strain-matched Grin3a knockout mice. *Alzheimers Dement*. 2023;19(9):4264-4266. doi:10.1002/ALZ.13375
33. Allen B, Ingram E, Takao M, et al. Abundant tau filaments and nonapoptotic neurodegeneration in transgenic mice expressing human P301S tau protein. *J Neurosci*. 2002;22(21):9340-9351. doi:10.1523/JNEUROSCI.22-21-09340.2002
34. Borchelt DR, Ratovitski T, Van Lare J, et al. Accelerated amyloid deposition in the brains of transgenic mice coexpressing mutant presenilin 1 and amyloid precursor proteins. *Neuron*. 1997;19(4):939-945. doi:10.1016/S0896-6273(00)80974-5
35. Jankowsky JL, Fadale DJ, Anderson J, et al. Mutant presenilins specifically elevate the levels of the 42 residue beta-amyloid peptide in vivo: evidence for augmentation of a 42-specific gamma secretase. *Hum Mol Genet*. 2004;13(2):159-170. doi:10.1093/HMG/DDH019
36. Sanchez-Mut J V., Heyn H, Silva BA, et al. PM20D1 is a quantitative trait locus associated with Alzheimer's disease. *Nat Med*. 2018;24(5):598-603. doi:10.1038/S41591-018-0013-Y
37. Zhou X, Chen Z, Yun W, Ren J, Li C, Wang H. Extrasynaptic NMDA receptor in excitotoxicity: function revisited. *Neuroscientist*. 2015;21(4):337-344. doi:10.1177/1073858414548724
38. Yanamandra K, Kfoury N, Jiang H, et al. Anti-tau antibodies that block tau aggregate seeding invitro markedly decrease pathology and improve cognition in vivo. *Neuron*. 2013;80(2):402-414. doi:10.1016/j.neuron.2013.07.046
39. González-González IM, Gray JA, Ferreira J, et al. GluN3A subunit tunes NMDA receptor synaptic trafficking and content during postnatal brain development. *Cell Rep*. 2023;42(5):112477. doi:10.1016/J.CELREP.2023.112477
40. Groc L, Heine M, Cousins SL, et al. NMDA receptor surface mobility depends on NR2A-2B subunits. *Proc Natl Acad Sci U S A*. 2006;103(49):18769-18774. doi:10.1073/PNAS.0605238103
41. Martel MA, Wyllie DJA, Hardingham GE. In developing hippocampal neurons, NR2B-containing N-methyl-d-aspartate receptors (NMDARs) can mediate signaling to neuronal survival and synaptic potentiation, as well as neuronal death. *Neuroscience*. 2009;158(1):334-343. doi:10.1016/j.neuroscience.2008.01.080
42. Lai TW, Shyu WC, Wang YT. Stroke intervention pathways: NMDA receptors and beyond. *Trends Mol Med*. 2011;17(5):266-275. doi:10.1016/J.MOLMED.2010.12.008
43. Petralia RS. Distribution of extrasynaptic NMDA receptors on neurons. *ScientificWorldJournal*. 2012;2012:267120. doi:10.1100/2012/267120
44. Sattler R, Xiong Z, Lu WY, MacDonald JF, Tymianski M. Distinct roles of synaptic and extrasynaptic NMDA receptors in excitotoxicity. *J Neurosci*. 2000;20(1):22. doi:10.1523/JNEUROSCI.20-01-00022.2000
45. Huang YWA, Zhou B, Wernig M, Südhof TC. ApoE2, ApoE3, and ApoE4 differentially stimulate APP transcription and aβ secretion. *Cell*. 2017;168(3):427-441.e21. doi:10.1016/j.cell.2016.12.044
46. Parsons MP, Raymond LA. Extrasynaptic NMDA receptor involvement in central nervous system disorders. *Neuron*. 2014;82(2):279-293. doi:10.1016/J.NEURON.2014.03.030
47. Gladding CM, Raymond LA. Mechanisms underlying NMDA receptor synaptic/extrasynaptic distribution and function. *Mol Cell Neurosci*. 2011;48(4):308-320. doi:10.1016/J.MCN.2011.05.001
48. Papouin T, Oliet SHR. Organization, control and function of extrasynaptic NMDA receptors. *Philos Trans R Soc B Biol Sci*. 2014;369(1654):20130601. doi:10.1098/RSTB.2013.0601
49. Nakanishi N, Tu S, Shin Y, et al. Neuroprotection by the NR3A subunit of the NMDA receptor. *J Neurosci*. 2009;29(16):5260. doi:10.1523/JNEUROSCI.1067-09.2009
50. Lau SF, Cao H, Fu AKY, Ip NY. Single-nucleus transcriptome analysis reveals dysregulation of angiogenic endothelial cells and neuroprotective glia in Alzheimer's disease. *Proc Natl Acad Sci U S A*. 2020;117(41):25800-25809. doi:10.1073/PNAS.2008762117/-/DCSUPPLEMENTAL
51. Das S, Li Z, Wachter A, et al. Distinct transcriptomic responses to aβ plaques, neurofibrillary tangles, and APOE in Alzheimer's disease. *Alzheimers Dement*. 2024;20(1):74-90. doi:10.1002/alz.13387
52. Mathys H, Davila-Velderrain J, Peng Z, et al. Single-cell transcriptomic analysis of Alzheimer's disease. *Nature*. 2019;570(7761):332-337. doi:10.1038/S41586-019-1195-2
53. Bossers K, Wirz KTS, Meerhoff GF, et al. Concerted changes in transcripts in the prefrontal cortex precede neuropathology in Alzheimer's disease. *Brain*. 2010;133(Pt 12):3699-3723. doi:10.1093/BRAIN/AWQ258
54. Qian Z, Qin J, Lai Y, Zhang C, Zhang X. Large-scale integration of single-cell RNA-Seq data reveals astrocyte diversity and transcriptomic modules across six central nervous system disorders. *Biomolecules*. 2023;13(4):692. doi:10.3390/BIOM13040692
55. Sze CI, Bi H, Kleinschmidt-DeMasters BK, Filley CM, Martin LJ. N-Methyl-D-aspartate receptor subunit proteins and their phosphorylation status are altered selectively in Alzheimer's disease. *J Neurol Sci*. 2001;182(2):151-159. doi:10.1016/S0022-510X(00)00467-6
56. Bi H, Sze CI. N-methyl-D-aspartate receptor subunit NR2A and NR2B messenger RNA levels are altered in the hippocampus and

entorhinal cortex in Alzheimer's disease. *J Neurol Sci*. 2002;200(1-2):11-18. doi:10.1016/S0022-510X(02)00087-4
57. Mishizen-Eberz AJ, Rissman RA, Carter TL, Ikonomovic MD, Wolfe BB, Armstrong DM. Biochemical and molecular studies of NMDA receptor subunits NR1/2A/2B in hippocampal subregions throughout progression of Alzheimer's disease pathology. *Neurobiol Dis*. 2004;15(1):80-92. doi:10.1016/j.nbd.2003.09.016
58. Hynd MR, Scott HL, Dodd PR. Differential expression of N-methyl-D-aspartate receptor NR2 isoforms in Alzheimer's disease. *J Neurochem*. 2004;90(4):913-919. doi:10.1111/J.1471-4159.2004.02548.X
59. Zhang Q, Ma C, Chin LS, Pan S, Li L. Human brain glycoform coregulation network and glycan modification alterations in Alzheimer's disease. *Sci Adv*. 2024;10(14):eadk6911. doi:10.1126/SCIADV.ADK6911
60. Kaniakova M, Lichnerova K, Skrenkova K, Vyklicky L, Horak M. Biochemical and electrophysiological characterization of N-glycans on NMDA receptor subunits. *J Neurochem*. 2016:546-556. doi:10.1111/jnc.13679
61. Storey GP, Opitz-Araya X, Barria A. Molecular determinants controlling NMDA receptor synaptic incorporation. *J Neurosci*. 2011;31(17):6311-6316. doi:10.1523/JNEUROSCI.5553-10.2011
62. Schedin-Weiss S, Winblad B, Tjernberg LO. The role of protein glycosylation in Alzheimer disease. *FEBS J*. 2014;281(1):46-62. doi:10.1111/FEBS.12590
63. Conroy LR, Hawkinson TR, Young LEA, Gentry MS, Sun RC. Emerging roles of N-linked glycosylation in brain physiology and disorders. *Trends Endocrinol Metab*. 2021;32(12):980-993. doi:10.1016/J.TEM.2021.09.006
64. Zhang Q, Ma C, Chin L-S, Pan S, Li L. Human brain glycoform coregulation network and glycan modification alterations in Alzheimer's disease. *bioRxiv* [Preprint]. 2023:2023.11.13.566889. doi:10.1101/2023.11.13.566889
65. Bieberich E. Synthesis, processing, and function of N-glycans in N-glycoproteins. *Adv Neurobiol*. 2023;29:65-93. doi:10.1007/978-3-031-12390-0_3
66. Song XJ, Zhou HY, Sun YY, Huang HC. Phosphorylation and glycosylation of amyloid-β protein precursor: the relationship to trafficking and cleavage in Alzheimer's disease. *J Alzheimers Dis*. 2021;84(3):937-957. doi:10.3233/JAD-210337
67. Boix CP, Lopez-Font I, Cuchillo-Ibañez I, Sáez-Valero J. Amyloid precursor protein glycosylation is altered in the brain of patients with Alzheimer's disease. *Alzheimers Res Ther*. 2020;12(1):96. doi:10.1186/S13195-020-00664-9
68. Lennol MP, Sánchez-Domínguez I, Cuchillo-Ibañez I, et al. Apolipoprotein E imbalance in the cerebrospinal fluid of Alzheimer's disease patients. *Alzheimer's Res Ther*. 2022;14(1):161. doi:10.1186/s13195-022-01108-2
69. Botella-López A, Burgaya F, Gavín R, et al. Reelin expression and glycosylation patterns are altered in Alzheimer's disease. *Proc Natl Acad Sci U S A*. 2006;103(14):5573-5578. doi:10.1073/pnas.0601279103
70. Sáez-Valero J, Sberna G, McLean CA, Masters CL, Small DH. Glycosylation of acetylcholinesterase as diagnostic marker for Alzheimer's disease. *Lancet (London, England)*. 1997;350(9082):929. doi:10.1016/S0140-6736(97)24039-0
71. García-Ayllón MS, Botella-López A, Cuchillo-Ibañez I, et al. HNK-1 carrier glycoproteins are decreased in the Alzheimer's disease brain. *Mol Neurobiol*. 2017;54(1):188-199. doi:10.1007/s12035-015-9644-x
72. Nakazawa T, Komai S, Tezuka T, et al. Characterization of Fyn-mediated tyrosine phosphorylation sites on GluR epsilon 2 (NR2B) subunit of the N-methyl-D-aspartate receptor. *J Biol Chem*. 2001;276(1):693-699. doi:10.1074/JBC.M008085200
73. Gong CX, Liu F, Grundke-Iqbal I, Iqbal K. Impaired brain glucose metabolism leads to Alzheimer neurofibrillary degeneration through a decrease in tau O-GlcNAcylation. *J Alzheimers Dis*. 2006;9(1):1-12. doi:10.3233/JAD-2006-9101
74. Alfaro-Ruiz R, Aguado C, Martín-Belmonte A, et al. Different modes of synaptic and extrasynaptic NMDA receptor alteration in the hippocampus of P301S tau transgenic mice. *Brain Pathol*. 2023;33(1):e13115. doi:10.1111/bpa.13115
75. Xu L, Zhou Y, Hu L, et al. Deficits in N-methyl-D-aspartate receptor function and synaptic plasticity in hippocampal CA1 in APP/PS1 mouse model of Alzheimer's disease. *Front Aging Neurosci*. 2021;13:772980. doi:10.3389/FNAGI.2021.772980
76. He RB, Li L, Liu LZ, et al. Ceftriaxone improves impairments in synaptic plasticity and cognitive behavior in APP/PS1 mouse model of Alzheimer's disease by inhibiting extrasynaptic NMDAR-STEP61 signaling. *J Neurochem*. 2023;166(2):215-232. doi:10.1111/JNC.15874
77. Rammes G, Mattusch C, Wulff M, et al. Involvement of GluN2B subunit containing N-methyl-d-aspartate (NMDA) receptors in mediating the acute and chronic synaptotoxic effects of oligomeric amyloid-beta (Aβ) in murine models of Alzheimer's disease (AD). *Neuropharmacology*. 2017;123:100-115. doi:10.1016/J.NEUROPHARM.2017.02.003
78. Salter MW, Pitcher GM. Dysregulated Src upregulation of NMDA receptor activity: a common link in chronic pain and schizophrenia. *FEBS J*. 2012;279(1):2-11. doi:10.1111/J.1742-4658.2011.08390.X
79. Barki-Harrington L, Elkobi A, Tzabary T, Rosenblum K. Tyrosine phosphorylation of the 2B subunit of the NMDA receptor is necessary for taste memory formation. *J Neurosci*. 2009;29(29):9219-9226. doi:10.1523/JNEUROSCI.5667-08.2009
80. Waters EM, Mazid S, Dodos M, et al. Effects of estrogen and aging on synaptic morphology and distribution of phosphorylated Tyr1472 NR2B in the female rat hippocampus. *Neurobiol Aging*. 2019;73:200-210. doi:10.1016/J.NEUROBIOLAGING.2018.09.025

SUPPORTING INFORMATION

Additional supporting information can be found online in the Supporting Information section at the end of this article.

How to cite this article: Escamilla S, Badillos R, Comella JX, et al. Synaptic and extrasynaptic distribution of NMDA receptors in the cortex of Alzheimer's disease patients. *Alzheimer's Dement*. 2024;20:8231–8245. https://doi.org/10.1002/alz.14125